

Influence of annealing parameters on the ferromagnetic properties of optimally passivated (Ga,Mn)As epilayers

V. Stanciu,^{1,*} O. Wilhelmsson,² U. Bexell,³ M. Adell,⁴ J. Sadowski,⁵ J. Kanski,⁴ P. Warnicke,¹ and P. Svedlindh¹

¹Department of Engineering Sciences, Uppsala University, Box 534, SE-751 21 Uppsala, Sweden

²Department of Material Chemistry, Uppsala University, Box 538, SE-751 21 Uppsala, Sweden

³Dalarna University, SE-781 88 Borlänge, Sweden

⁴Department of Experimental Physics, Chalmers University of Technology, SE-41296 Göteborg, Sweden

⁵Institute of Physics, Polish Academy of Sciences, PL-02668 Warszawa, Poland

(Dated: August 30, 2018)

The influence of annealing parameters - temperature (T_a) and time (t_a) - on the magnetic properties of As-capped (Ga,Mn)As epitaxial thin films have been investigated. The dependence of the transition temperature (T_C) on t_a marks out two regions. The T_C peak behavior, characteristic of the first region, is more pronounced for thick samples, while for the second ('saturated') region the effect of t_a is more pronounced for thin samples. A right choice of the passivation medium, growth conditions along with optimal annealing parameters routinely yield T_C -values of ~ 150 K and above, regardless of the thickness of the epilayers.

PACS numbers: 75.50.Pp, 75.30.Gw, 75.70.-i

Tremendous experimental and theoretical work has recently been dedicated to the study of III-V diluted magnetic semiconductors (DMS). Particularly (Ga,Mn)As has received sustained interest because of its relatively high ferromagnetic transition temperature, being regarded as the prototype of this new class of materials [1, 2]. However, device applications call for further improvements of its magnetic properties.

In this compound, the Mn impurities ideally substitute on Ga sites and occupy random positions in the GaAs matrix. The substitutional Mn cation (Mn_{Ga}) has a double role in the lattice host; it acts as a magnetic ion (its five 3d electrons do not participate in the bonding) and as an acceptor yielding one hole in the GaAs matrix. The magnetic interactions between the magnetic ions are mediated by the free holes. A common point in all theoretical descriptions of ferromagnetism in these systems is that the ferromagnetic (FM) order has a direct correspondence to the net dopant and hole concentration, x and p , respectively. The latter is very sensitive to the level of compensating defects. High Mn concentrations require the MBE growth to be performed at low temperatures (LT) and, due to this special growth condition, native LT-GaAs defects [3] are incorporated during the deposition process. One such defect is the As antisite (As_{Ga}), i.e., As atoms substituting in the Ga sublattice. As_{Ga} is a double donor. Hence, it compensates two Mn_{Ga} and therefore has a negative impact on the ferromagnetic properties [4]. Mn atoms sitting in the tetrahedrally As-coordinated interstitial positions (Mn_I) [5] in the zincblende structure of GaAs form another important type of defect [6, 7]. Mn_I is also a double donor [8] and besides this, its d orbitals do not hybridize with the p states of the holes in the valence band and therefore do not participate in the hole-induced ferromagnetism [9]. Moreover, it was shown in Ref. [9] that Mn_I couples antiferromag-

netically by a superexchange mechanism with the nearest Mn_{Ga} . Both As_{Ga} and Mn_I cause a decrease of the hole concentration and the manganese magnetic moment [4, 10].

A key issue for the improved magnetic properties recently reported [11, 12, 13, 14] is the 'optimal' LT annealing. There are three important annealing parameters; the annealing environment, the annealing time (t_a) and the annealing temperature (T_a). In most of the annealing studies performed hitherto, only one of these parameters is varied, while the others are considered 'optimal'. Because of these narrow experimental parameter windows there is no consensus on what should be regarded as 'optimal' annealing conditions. Concerning the annealing environment, annealings have been performed either in-situ (in the deposition chamber, immediately after the growth) [15] or under the flow of a gas stream, e.g. pure N_2 [16, 17] or O_2 [18], or in air [12, 14]. Most of these procedures, particularly if performed at low T_a , are lengthy, i.e., they require extended annealing times to yield noticeable improvements of the magnetic properties. The annealing temperatures are regarded as 'low' (e.g., 170 °C [11]) or 'high' (e.g., more than 300 °C [16]) when compared to the growth temperature (T_g). Therefore, when defining a reference for T_a , one should always take into consideration the growth conditions, especially T_g [19]. The annealing time, somehow following the conditions 'low T_a - long t_a ' or vice versa, has been varied between a few minutes to many days. Here, we show that a proper balance between T_a , t_a and, not the least, the annealing environment may give a sense to what optimal annealing conditions are.

The mechanism behind the large increase of T_C (of the as-grown samples) is the out-diffusion of the highly mobile Mn_I [7] to the free surface of the (Ga,Mn)As epilayer, followed by their passivation in this region [14]. Here,

we choose as a reactive medium a comparably thick cap layer of amorphous As (*a*-As). Passivation of the freshly grown surfaces by capping with an amorphous As layer is a well known procedure for pure semiconductors [20, 21]. In case of (Ga,Mn)As, the efficiency of the *a*-As cap as regards Mn_I passivation has recently been addressed in Ref. [22].

This study focuses on $Ga_{1-x}Mn_xAs$ layers with Mn concentrations of $x \sim 0.05$ and 0.06 . The chosen range of x has proved to give the best magnetic properties [11]. The study does not cover the ultrathin thickness range, nor does it cover very thick layers - the film thickness in this study varies between 100 \AA to 1000 \AA . LT-MBE growth was employed and for the range of doping concentrations mentioned above, T_g was about $230 \text{ }^\circ\text{C}$. Further details on the sample preparation are found elsewhere [22]. The $1 \times 1 \text{ cm}^2$ as-grown samples were cleaved in many small pieces necessary for subsequent post-growth annealings. The LT annealings were performed in air in a closed oven (accuracy $\pm 3 \text{ }^\circ\text{C}$). The annealing temperatures (either higher or lower than T_g) ranged from $150 \text{ }^\circ\text{C}$ to $300 \text{ }^\circ\text{C}$.

Time-of-flight secondary ion mass spectrometry (ToF-SIMS) was performed with a PHI TRIFT II instrument using a pulsed 15 kV liquid metal ion source enriched in $^{69}\text{Ga}^+$ ions. Depth profiles were obtained by sputtering a surface area of $50 \times 50 \mu\text{m}^2$ and measure on an analysing area of $25 \times 25 \mu\text{m}^2$. To enhance the secondary ion emission the depth profiles were measured under oxygen flooding with a base pressure of 10^{-6} Torr in the sample chamber. The sputter-rate was determined from the full-width at half-maximum of the Mn-profile for the (Ga,Mn)As layer.

Chemical analyses of the films were performed by X-ray photoelectron spectroscopy (XPS) using a Phi Quantum 2000 instrument with monochromatized Al $K\alpha$ radiation with an accuracy of $\pm 0.1 \text{ eV}$. Peaks from As($3d$), Ga($2p$), Mn($2p$) and Mn($3p$) were analysed to settle the chemical state. To compensate any drift in the binding energy between the samples, due to charging effects, the C($1s$) peak was measured for all films and positioned at 285.1 eV .

The magnetic measurements were performed in a QuantumDesign MPMS-XL Superconducting QUantum Interference Device (SQUID) magnetometer. The ferromagnetic transition temperatures were derived from the temperature dependence of the magnetization, $M(T)$, as the onset of the FM order. For consistency, the $M(T)$ measurements were performed in a low magnetic field (20 Oe) (field-cooled protocol) applied in the film-plane along either $[110]$ or $[-110]$ directions. $[110]$ direction turns to be the easy axis (*EA*) of magnetization for all annealed samples, while the as-grown samples show an *EA* along $[-110]$ [23]. Fig. 1 (b) and (c) show examples of $M(T)$ measurements recorded along the *EA* for two different

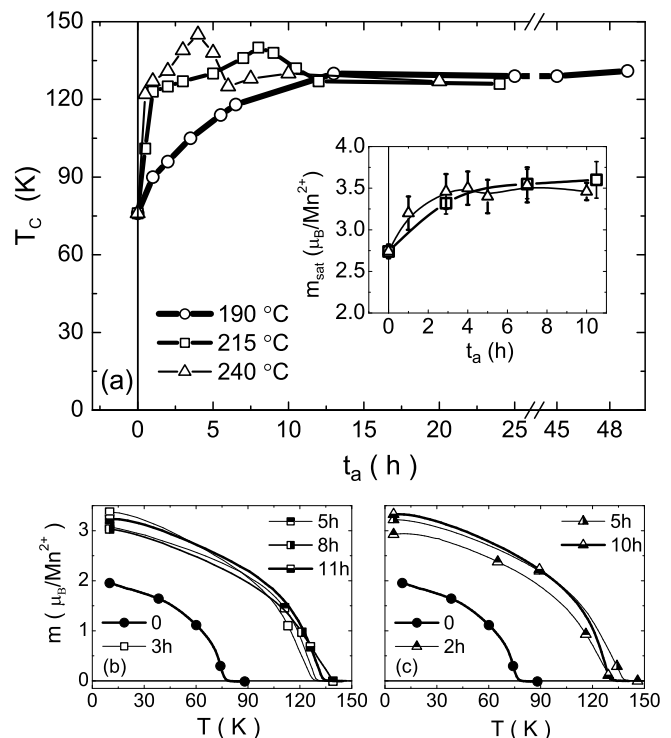


FIG. 1: (a) T_C vs. annealing time for the 1000 \AA thick film. The inset shows the variation of the saturation magnetic moment with t_a . (b) and (c) show the Brillouin-like $M(T)$ curves recorded at $T_a = 215 \text{ }^\circ\text{C}$ and $240 \text{ }^\circ\text{C}$, respectively (the as-grown sample is denoted by ‘0’).

annealing temperatures. In Fig. 1 (a), taking T_a as a parameter, the dependence of T_C of a 1000-\AA -thick sample on annealing time is shown. Two T_a -dependent regions can be identified; the first region is characterized by a peak in T_C at $\sim 4 \text{ h}$ and 7 h for the annealing temperatures $240 \text{ }^\circ\text{C}$ and $215 \text{ }^\circ\text{C}$, respectively, while for $T_a = 190 \text{ }^\circ\text{C}$ there is a gradual increase of T_C with annealing time. The second region occurs for t_a longer than $\sim 10 \text{ h}$ and is characterized, for both *high* (but below $250\text{--}260 \text{ }^\circ\text{C}$) and *low* T_a , by a slight decrease of T_C (by a few K), more pronounced at higher T_a and practically unnoticeable at $T_a = 190 \text{ }^\circ\text{C}$ and below. One may however regard this region of the t_a -dependence as a ‘saturated’ region provided T_a is not too high or, if T_a is higher than T_g , t_a does not exceed certain limits (e.g., several tens of hours at $240 \text{ }^\circ\text{C}$). For annealing temperatures close to T_g , the slight decay of T_C in the second region is negligible as compared to the results presented in Ref. [17]. At these T_a ’s the Mn_I out-diffusion process practically ends after few hours of annealing and what follows is merely a re-configuration of the interface region, as we discuss below.

The inset of Fig. 1 (a) shows the dependence of the manganese magnetic moment, derived at magnetic saturation, on annealing time. When calculating the mag-

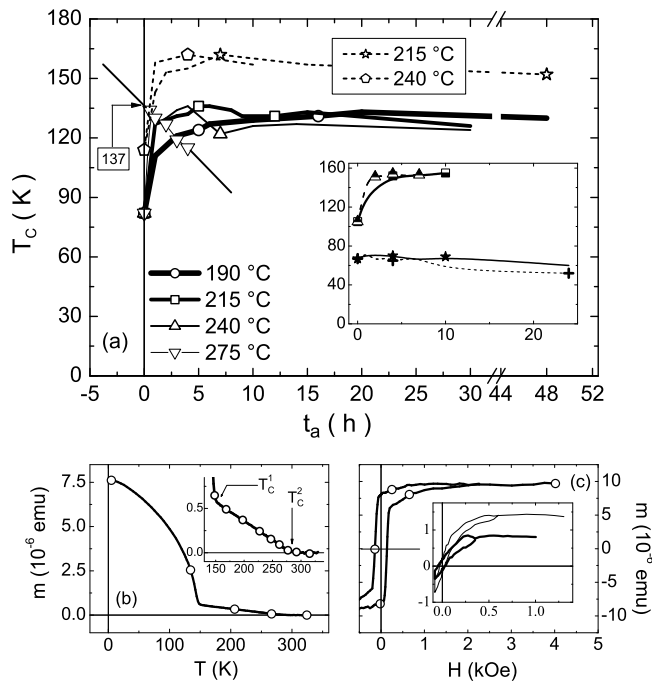


FIG. 2: (a) T_C vs. annealing time for 300 Å (solid lines) and 500 Å (dashed lines) thick samples with $x \sim 6\%$ Mn. The inset shows a comparison between two 400 Å thick samples, capped with a -As and GaAs, as indicated. (b) $M(T)$ for one of the a -As capped 400-Å-thick samples annealed at 275 °C for 15 minutes. The inset shows a zoomed portion of the $M(T)$ curve. (c) $M(H)$ at $T = 5$ K for the same sample as in (b), the corresponding results at $T = 200$ K and 250 K are shown in the inset.

netic moment per Mn atom, we do not consider the change of the Mn concentration within the bulk of the (Ga,Mn)As layer, which results from the annealing-induced depletion process. If this effect was considered, the magnetic moments would be close to the expected $4\mu_B/\text{Mn-atom}$ [4]. As one may notice, there is a monotonous increase of m_{sat} without any special features at t_a corresponding to the T_C -peaks. Due to the nonequilibrium growth conditions of LT-MBE, the top-surface of the (Ga,Mn)As layer becomes enriched in Mn, mostly Mn_I , during the deposition [8, 24]. This is also confirmed by our ToF-SIMS measurements on as-grown samples; the Mn depth-profile reveals an increase in manganese concentration close to the a -As/(Ga,Mn)As interface. In subsequent annealings, the excess Mn at the interface may play the role of nucleation centers for a presumed island growth of a Mn-As compound. At sufficiently large T_a , four processes may be identified; (1) diffusion of Mn_I from the film towards the substrate interface (a process that does not enhance the ferromagnetic properties as the GaAs cannot passivate Mn_I) [see inset of Fig. 2 (a), where it is shown that LT-annealing has no significant effect on a (Ga,Mn)As film capped with 100 Å of GaAs], (2) diffusion towards the film/cap in-

terface, (3) migration of Mn_I at the interface, and (4) an eventual diffusion of Mn_I into the a -As cap. In parallel, desorption of the a -As cap takes place, at a rate that is also T_a -dependent. Mn_I 's reaching the film/cap interface are passivated by reacting with the a -As cap. Initially, heterogeneous, non-stoichiometric 2D-islands of Mn-As are formed. During the first few hours of annealing, these islands grow laterally rather than vertically, while for longer annealing times, close to the t_a peak-values (t_a^{peak}), diffusion of Mn_I into the a -As cap may also take place. Thus, the $\text{Ga}_{1-x}\text{Mn}_x\text{As}/a$ -As interface has a double role; (i) it efficiently accommodates out-diffused Mn_I 's and (ii) for a certain interface coverage, it rises, though 'artificially', T_C of the underlying structure, hence leading to the appearance of the T_C -peaks. However, as the a -As cap desorbs, the MnAs interface compound decomposes and a manganese-oxide layer is gradually formed. The initial 'equilibrium', which brought the T_C to the peak-values, is now broken and this is signaled by the decrease of T_C within 1-2 hours after the t_a^{peak} 's. A new steady state at the surface is reached, corresponding to the second t_a -region mentioned above, this time in the presence of a comparably thick manganese-oxide/arsenic-oxide layer characterized by an almost constant value of T_C . It should be emphasized that the drop in T_C is not due to O_2 or N_2 contamination, since it has been shown in other LT-annealing studies that both O_2 and N_2 have a positive effect on the magnetic properties [13, 14, 18], but is due to the partial 'alteration' of the particular state created by the MnAs structure at the interface. A few more arguments in favor of the above statements can be given: (i) The saturation magnetic moment does not change after the first few hours of annealing, implying that the annealing process (bulk diffusion) ends rather quickly; (ii) by careful annealing at high T_a for a few minutes only, the MnAs 'layer' can be 'caught' intact at the interface [25]. This 'layer' may be composed of either large islands perhaps forming a percolating network or it may be a continuous thin MnAs layer. In Fig. 2 (b) and (c), the $M(T)$ and $M(H)$ results are shown for a 400 Å thick sample annealed at 275 °C for 15 minutes. As we see from the $M(T)$ dependence, the (Ga,Mn)As film does not appear inhomogeneous [26], i.e., we exclude the possibility of having a phase separation (MnAs clusters or precipitates) within the bulk of (Ga,Mn)As. This is also certified by the high T_C value (~ 150 K) obtained for the (Ga,Mn)As (denoted T_C^1) and also by the shape of the $M(H)$ curve at $T = 5$ K. The latter measurement was recorded after cooling the sample to 5K in an applied field of 30 kOe. There is no indication of a presumed exchange-bias shift of the hysteresis loop, therefore the top layer is ferromagnetic which in this case may fit a MnAs compound. The saturation magnetization extracted from $M(H)$ for $T > T_C^1$, assuming a continuous layer of MnAs at the interface, would correspond to a layer thickness of 2 nm [27]. A

second transition (T_C^2) occurs at ~ 280 K as seen in the inset of Fig. 2 (b), which is in good agreement with the ferromagnetic ordering temperature previously observed for nanoscale MnAs dots [28].

The situation changes for thin layers. In Fig. 2 (a), T_C vs. t_a for a series of thin samples (300 Å, 400 Å and 500 Å) is shown. A detailed annealing study was only performed for the 300 Å thick series, while for the other thicknesses the aim was to obtain T_C -values at the already established t_a^{peak} 's. Comparing the results for the 300 Å and 1000 Å (cf. Fig. 1) thick samples, it can be seen that the T_C -peak behavior is less pronounced for the thinner sample. The difference between the T_C -peak values and the 'plateau' value of the second region is very small. Moreover, the effect of *high* T_a is stronger causing a more accelerated degradation of the bulk (Ga,Mn)As ferromagnetic properties. One may therefore conclude that thinner samples are more quickly depleted from Mn_I and that the special interface state appearing as a result of the depletion exhibits [Mn]-dependent properties. This implies that for a more thick sample, the number of Mn_I reaching the interface is larger, yielding larger 2D-islands of MnAs and for thick enough samples a full layer of MnAs is formed at the interface.

Some samples presented in Fig. 1 were subjected to ToF-SIMS and XPS analyses. First, the as-grown surface was investigated. For $T_a = 215^\circ\text{C}$ and $t_a \leq 3$ h, the XPS results indicate only the presence of elemental As and As-O at the top surface. However, for $t_a = 7$ h, Mn(2p) and Mn(3p) peaks were identified as coming from Mn-O and Mn-As. Due to expected small peak-shifts, it is difficult to separate the Mn-O/Mn-As peaks, but it is clear from the $M(T)$ results (cf. e.g. Fig. 2 (b)) that MnAs is also present. Even after 12 h of annealing the elemental As peak is still present, though at a smaller concentration as compared to the case of shorter t_a . There is a weak Ga peak, indicating a desorbed cap and a thickness of the cap remains comparable to the XPS photoelectron escape depth, ~ 40 Å. The intensity of the Mn-O/Mn-As peak does not change much in comparison to the up-or-down change of the intensity for the As-O and As-As peaks - the longer the t_a the smaller the As-As peak becomes while the As-O peak increases in magnitude.

Manganese depth-profiles obtained from ToF-SIMS measurements on 1000 Å thick, *a*-As capped (Ga,Mn)As films are shown in Fig. 3; the different curves refer to different t_a at $T_a = 240^\circ\text{C}$. The depth profiles clearly show that Mn_I exhibits a net diffusion towards the *a*-As/(Ga,Mn)As interface and that Mn_I is passivated at this interface. For $T_a = 240^\circ\text{C}$, the cap is completely desorbed after $\sim 1 - 2$ h of annealing, while it takes $\sim 3 - 4$ h of annealing at $T_a = 215^\circ\text{C}$ for the cap to desorb. After cap desorption, there are only minute changes in the Mn depth-profile with increasing annealing time; the thickness of the passivation layer, consisting of Mn-O/Mn-As, is estimated to be ~ 60

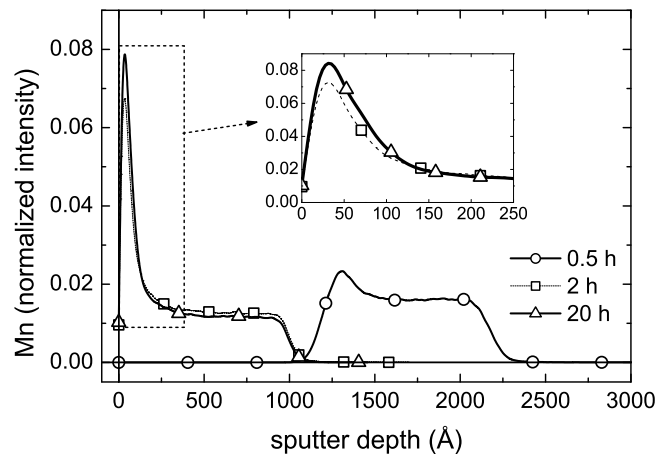


FIG. 3: Mn depth-profiles for 1000 Å thick, *a*-As capped (Ga,Mn)As films. The different curves correspond to different t_a at $T_a = 240^\circ\text{C}$; circles $t_a = 0.5$ h, squares $t_a = 2$ h and, triangles $t_a = 20$ h.

Å from the full-width half-maximum of Mn-peak at small sputtering depth. The stability of the T_C -peaks is to some extent limited by the thickness of the *a*-As cap. This can be an explanation for the difference between the results presented here and the results of Ref. [22], where slightly different growth conditions were employed (e.g., a smaller cap thickness was used). The apparent positive effect of the MnAs layer manifests only by a small increase of the carrier concentration, as the Mn dopant concentration decreases during the annealing process.

In summary, the influence of different annealing parameters on T_C of (Ga,Mn)As epilayers (different thicknesses but constant x) has been described. For annealing temperatures close to T_g relatively short annealing times are required for a complete Mn_I depletion of both thin and thick samples. This proves the efficiency of the *a*-As cap and emphasizes the crucial role played by the *a*-As/(Ga,Mn)As interface in controlling both the diffusion process within the bulk of (Ga,Mn)As and the peculiar behavior of the magnetic properties that follows after the completion of this diffusion process. Moreover, it has been shown that; (i) For a particular choice of the annealing parameters a ferromagnetic MnAs structure can be obtained at the interface; (ii) the impairment of the ferromagnetic properties is much less pronounced while using the *a*-As-cap as compared to case of 'free' (Ga,Mn)As surfaces exposed either to air, N_2 or O_2 during the LT-annealing process.

The Swedish Foundation for Strategic Research (SSF) and the Swedish Research Council (VR) are acknowledged for financial support.

-
- * Electronic address: victor.stanciu@angstrom.uu.se
- [1] H. Ohno and F. Matsukura, *Solid State Commun.* **117**, 179 (2001).
- [2] A. H. MacDonald, P. Schiffer, and N. Samarth, *Nature Materials* **4**, 195 (2005).
- [3] X. Liu, A. Prasad, E. R. Weber, Z. Liliental-Weber, and W. Walukiewicz, *Appl. Phys. Lett.* **67**, 279 (1995).
- [4] P. A. Korzhavyi, I. A. Abrikosov, E. A. Smirnova, L. Bergqvist, P. Mohn, R. Mathieu, P. Svedlindh, J. Sadowski, E. I. Isaev, Y. K. Vekilov, et al., *Phys. Rev. Lett.* **88**, 187202 (2002).
- [5] F. Glas, G. Patriarche, L. Largeau, and A. Lemaitre, *Phys. Rev. Lett.* **93**, 086107 (2004).
- [6] F. Maca and J. Masek, *Phys. Rev. B* **65**, 235209 (2002).
- [7] K. M. Yu, W. Walukiewicz, T. Wojtowicz, I. Kuryliszyn, X. Liu, Y. Sasaki, and J. K. Furdyna, *Phys. Rev. B* **65**, 201303 (2002).
- [8] S. C. Erwin and A. G. Petukhov, *Phys. Rev. Lett.* **89**, 227201 (2002).
- [9] J. Blinowski and P. Kacman, *Phys. Rev. B* **67**, 121204 (2003).
- [10] K. Y. Wang, K. W. Edmonds, R. P. Champion, B. L. Gallagher, N. R. S. Farley, C. T. Foxon, M. Sawicki, P. Boguslawski, and T. Dietl, *J. Appl. Phys.* **95**, 6512 (2004).
- [11] K. W. Edmonds, K. Y. Wang, R. P. Champion, A. C. Neumann, N. R. S. Farley, B. L. Gallagher, and C. T. Foxon, *Appl. Phys. Lett.* **81**, 4991 (2002).
- [12] D. Chiba, K. Takamura, F. Matsukura, and H. Ohno, *Appl. Phys. Lett.* **82**, 3020 (2003).
- [13] K. C. Ku, S. J. Potashnik, R. F. Wang, S. H. Chun, P. Schiffer, N. Samarth, M. J. Seong, A. Mascarenhas, E. Johnston-Halperin, R. C. Myers, et al., *Appl. Phys. Lett.* **82**, 2302 (2003).
- [14] K. W. Edmonds, P. Boguslawski, K. Y. Wang, R. P. Champion, S. N. Novikov, N. R. S. Farley, B. L. Gallagher, C. T. Foxon, M. Sawicki, T. Dietl, et al., *Phys. Rev. Lett.* **92**, 37201 (2004).
- [15] A. Pross, S. Bending, K. Edmonds, R. P. Champion, C. T. Foxon, and B. Gallagher, *J. Appl. Phys.* **95**, 3225 (2004).
- [16] T. Hayashi, Y. Hashimoto, S. Katsumoto, and Y. Iye, *Appl. Phys. Lett.* **78**, 1691 (2001).
- [17] S. J. Potashnik, K. C. Ku, S. H. Chun, J. J. Berry, N. Samarth, and P. Schiffer, *Appl. Phys. Lett.* **79**, 1495 (2001).
- [18] M. Malfait, J. Vanacken, V. V. Moshchalkov, W. Van Roy, and G. Borghs, *Appl. Phys. Lett.* **86**, 132501 (2005).
- [19] x might also dictate what annealing conditions one has to choose, however, because of its strong T_g dependence, specifying T_g is usually enough.
- [20] S. P. Kowalczyk, D. L. Miller, J. R. Waldrop, P. G. Newman, and R. W. Grant, *J. Vac. Sci. Technol.* **19**, 255 (1981).
- [21] C. Heinlein, B. Fimland, J. K. Grepstad, and T. Berge, *J. Vac. Sci. Technol. B* **17**, 217 (1999).
- [22] M. Adell, L. Ilver, J. Kanski, V. Stanciu, P. Svedlindh, J. Sadowski, J. Z. Domagala, F. Terki, C. Hernandez, and S. Charar, *Appl. Phys. Lett.* **86**, 112501 (2005).
- [23] V. Stanciu and P. Svedlindh, (to be published).
- [24] K. M. Yu, W. Walukiewicz, T. Wojtowicz, J. Denlinger, M. A. Scarpulla, X. Liu, and J. Furdyna, *Appl. Phys. Lett.* **86**, 42102 (2005).
- [25] The XPS surface analysis shows only elemental As and As-O after $t_a = 20$ min at $T_a = 275$ °C.
- [26] R. Mathieu, B. S. Sorensen, J. Sadowski, U. Sodervall, J. Kanski, P. Svedlindh, P. E. Lindelof, D. Hrabovsky, and E. Vanelle, *Phys. Rev. B* **68**, 184421 (2003).
- [27] M. Tanaka, J. P. Harbison, M. C. Park, Y. S. Park, T. Shin, and G. M. Rothberg, *J. Appl. Phys.* **76**, 6278 (1994).
- [28] K. Ono, J. Okabayashi, M. Mizuguchi, M. Oshima, A. Fujimori, and H. Akinaga, *J. Appl. Phys.* **91**, 8088 (2002).